Available online at www.sciencedirect.com
ScienceDirect
Polymer 49 (2008) 1629–1634
polymer
www.elsevier.com/locate/polymer

Fractal crystal growth of poly(ethylene oxide) crystals from its amorphous monolayers

Zhenpeng Ma, Guoliang Zhang, Xuemei Zhai[1], Liuxin Jin, Xiongfeng Tang, Miao Yang, Ping Zheng, Wei Wang*

Key Laboratory of Functional Polymer Materials and Institute of Polymer Chemistry, College of Chemistry, Nankai University, Tianjin 300071, China

Received 11 November 2007; received in revised form 23 January 2008; accepted 24 January 2008
Available online 3 February 2008

Abstract

The fractal crystal growth process of the PEO monolayer with a molecular weight ($\overline{M}_w \approx 2.0 \times 10^6$ g/mol) and a distribution ($\overline{M}_w/\overline{M}_n = 4.24$) has been followed on the substrate of the silicon wafer using AFM equipped with a hot stage. A depletion zone between the ramified crystals and the viscous amorphous layer was found in the AFM height images. The formation of the depletion zone shows that the molecules have to ''break up'' with the amorphous layer and then diffuse through the depletion zone to join the crystals. The diffusion process further means the diffusion-controlled mechanism resulting in the fractal crystal pattern with a fractal dimension $D_f \approx 1.63$. The linear feature of the crystal pattern radius growth with time means that the surface kinetic process plays a key role in the crystal growth.

Keywords: Polymer crystallization; Monolayers; Crystal pattern formation

1. Introduction

The crystallization of linear polymers can be one of the most intriguing things in polymer science. Due to long chain nature, polymer crystallization and melting are much more complex than those of small molecules [1–3]. Under supercooling conditions polymers kinetically have to fold back and forth for several times to form folded-chain lamellar crystals, whose thickness is normally less than the contour length of the whole molecule. Normally, folded-chain crystals further organize into spherulites or, sometimes, larger single crystals with different shapes or patterns, highly dependent on crystallization conditions. For thin film samples the crystallization occurs in quasi-two-dimensional space so they can become more complex mainly due to the interaction between macromolecules and solid substrates.

At the supercooling condition, different crystal patterns have been found due to instability of crystal growth caused by a diffusion field [4,5]. The diffusion limited aggregation (DLA) mechanism [6] has attracted great attentions because as a fundamental model for pattern growth it can provide a basic understanding on the formation of complex aggregates with different shapes that have been found in the experiments of physics, chemistry, material science, and biology [7–20]. In the cases of considering boundary conditions [21–31], then different patterns, such as dendrite, seaweed (or densely branched morphology), and compact structure have been simulated, so the formation process and mechanism of the similar patterns, which were also found in experiments, can be more precisely explored.

The patterns of monolayers (or ultrathin films) of crystalline polymers have also been studied [13–20]. In 1964, Keith and Padden have reported their findings of lamellar crystals with branched pattern formed by folded-chain crystals of an isotactic polypropylene (PP) in a matrix of an atactic PP [13]. In 1984, Lovinger and Cais found the seaweed pattern in the ultrathin samples of a poly(trifluoroethylene) and were the first to employ DLA to qualitatively explain the formation

* Corresponding author. Fax: +86 22 2349 8126.
E-mail address: weiwang@nankai.edu.cn (W. Wang).
[1] Present address: Microscopy/Thermal Analytical Science, Asia Pacific Research, Dow Chemical (China) Investment Co. Ltd., 5/F, No. 512 Yutang Road Building C, Songjiang Industrial Park, Shanghai 201613, China.

0032-3861/$ - see front matter © 2008 Elsevier Ltd. All rights reserved.
doi:10.1016/j.polymer.2008.01.067

mechanism [10]. Recently, Reiter and Sommer observed liquid-like patterns in poly(ethylene oxide) (PEO) crystalline monolayers and employed the DLA model to simulate the process in order to explain the formation mechanism [15,16]. Similar patterns were also found in other crystalline polymers [17,19] or their blends [18]. In our previous work, we prepared monolayers of a PEO ($\overline{M}_w = 5.0 \times 10^3$ g/mol and $\overline{M}_w/\overline{M}_n = 1.01$) being more universal and then followed pattern transitions of this PEO monolayer with the increasing crystallization temperatures from nonequilibrium to near equilibrium [20]. These works provide us insights into the crystallization behavior and transitions of crystalline polymers in quasi-two-dimensions. However, the study on the growth of the fractal patterns of crystalline polymers is extremely rare [17,19].

In this work, we would like to report our in situ observation of the growth process of fractal crystals of PEO monolayers in a nonequilibrium condition. Our experiment will for the first time reveal a depletion zone existing in the area between the growing tip of the crystal pattern and the viscous amorphous layer in AFM height images. So, our discussion will focus on the migration process of PEO molecules through the depletion zone from the amorphous layer to the crystals to create the fractal patterns and the surface kinetic process of crystallization mainly on the growing tips to give rise to a linear feature of the pattern radius growth from the thin amorphous layer.

2. Experimental section

2.1. Materials and sample preparation

PEO sample, labeled as 200k, was purchased from J&K Chemicals. Its molecular weight was further determined by static laser scattering which was performed on a laser light scattering spectrometer (BI-200SM) equipped with a digital correlator (BI-9000AT) at a given temperature. Its absolute average molecular weight is $\overline{M}_w = 2.02 \times 10^5$ g/mol and the average radius of gyration, $\overline{R}_g$, in water is 50.2 nm. Using gel permeation chromatography (GPC Waters, calibrated by PEO samples) in *N*,*N*-dimethylformamide (DMF) solution, we obtained $\overline{M}_w = 2.18 \times 10^5$ g/mol and $\overline{M}_w/\overline{M}_n = 4.24$. Its ultimate equilibrium melting temperature, $T_m^0 = 68.8$ °C, was estimated using the method report in Ref. [32].

The monolayer samples for AFM studies were prepared as follows: the toluene solutions with a concentration of 0.01 wt % were prepared in glassware. The silicon wafers were cleaned in an ultrasonic water bath and then in an acetone bath. The thin PEO films on the surface of the silicon wafers were prepared simply by dropping the polymer solution at elevated temperature. The samples were dried at normal atmosphere overnight and then treated in a vacuum oven at room temperature for 12 h. Then a monolayer of lamellar crystals with fractal-like patterns formed on the surface of the silicon wafer. The cast samples were first heated to 75 °C for 5 min to let the lamellar crystals melt completely and then cooled to the selected temperature to let the polymer recrystallize.

2.2. Instruments

A hot-stage multimode atomic force microscope (Digital Instrumental Nanoscope IV) was used to visualize the pattern formation of PEO lamellar crystals. The temperature of the hot stage can be precisely controlled within ±0.1 °C. All measurements were performed in tapping mode. The temperature of the hot stage and the height determined were calibrated following the methods and using a standard sample provided by the manufacturer.

3. Results and discussion

3.1. Growth of fractal pattern

The PEO crystal pattern growth at 25 °C is shown in Fig. 1. (For the sake of getting the best resolution, variable image size scales are employed.) Clearly, all the crystal patterns have the typical seaweed feature with a tip-splitting head. The angles between main and side branches have no fixed value, and all the branches point out from the pattern centre to the outside zone where the amorphous macromolecules may come from. The widths of branches are much narrower comparing to the total length of each branch. When one branch grew to some extent, it generated new branches by splitting apart, and then both the parent branches and the newborn ones kept propagating. In this way the pattern gets larger and larger.

All the patterns basically have an approximately spherical symmetry. Their radii and areas were approximately measured as a function of time and the results are shown in Fig. 2. This graph shows that the radius plot has a good linear feature while the area plot is a parabolic one.

3.2. Depletion zone

An obvious depletion zone between the seaweed crystal pattern and the amorphous layer can be clearly seen. In order to visibly characterize the depletion zone, two surface profiles I and II, which are marked in Fig. 1(b), are displayed in Fig. 3. From the surface profiles the thickness of the amorphous layer is about 3 nm, while the thickness of the crystal pattern is about 8 nm. The formation of 3 nm thick amorphous layer should be due to a relatively strong attraction between the repeating units in PEO chains and hydroxyl groups on the silicon substrate. The PEO macromolecules in the amorphous layer have a ''pancake'' conformation [33].

To our best knowledge this is the first experimental evidence clearly showing a depletion zone in the AFM *height* images. From the surface profiles I and II shown in Fig. 3, we can see a relatively sharp edge between the amorphous layer and the depletion zone. This is because there is a great amount of entanglements among high molecular weight PEO chains. So, the PEO molecules in the viscous amorphous layer cannot easily flow into the depletion zone at the used temperature. The depletion zone around a dendritic pattern of PEO ($\overline{M}_w = 5.0 \times 10^4$ g/mol) was also found in the AFM *phase* images in a previous work [34]. The images show a phase difference

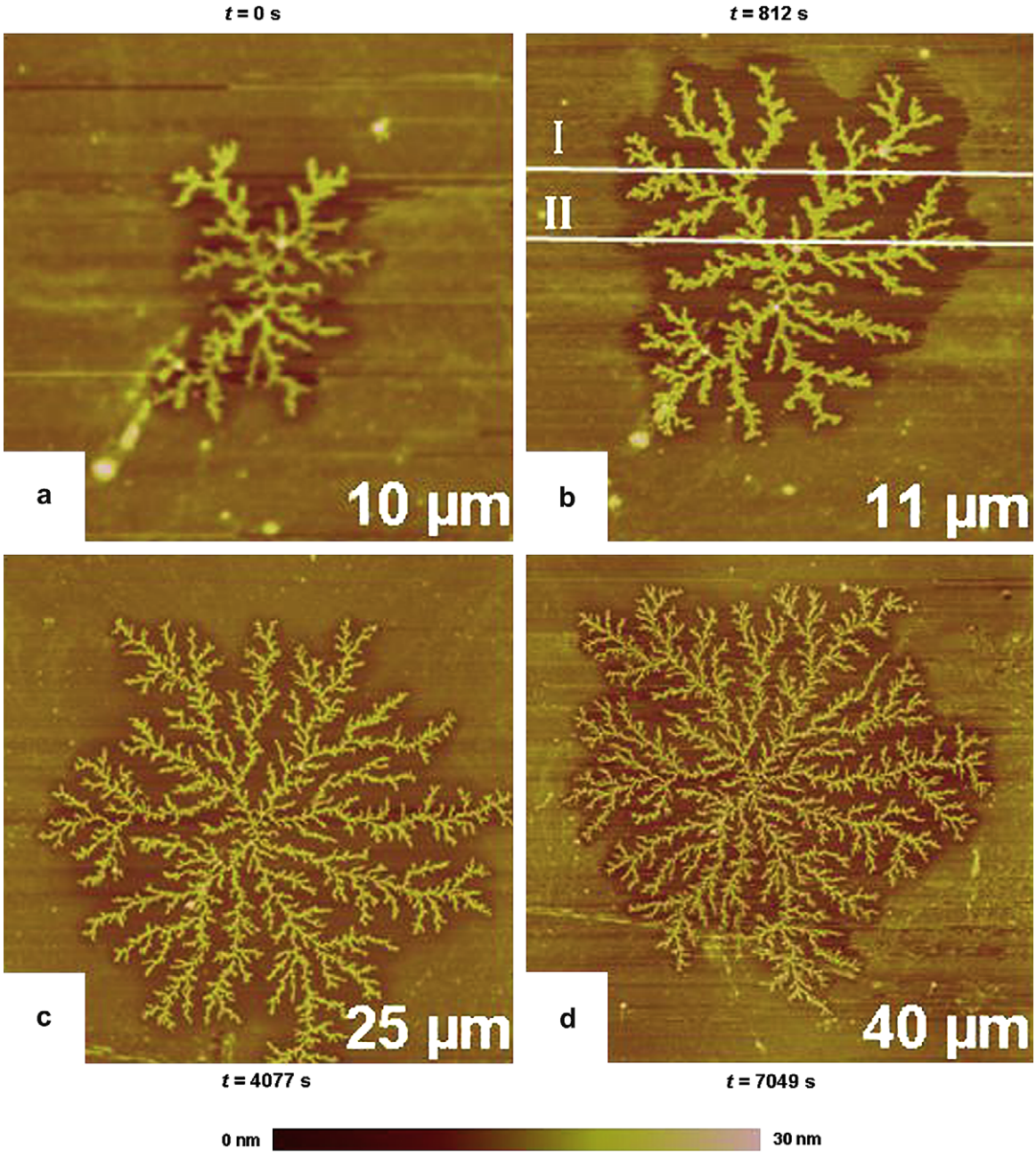

Fig. 1. AFM height images showing the growth process of a seaweed crystal pattern at 25 °C.

between crystal and molten polymer which gradually change in a length range of 1–2 μm. In other words, there is no sharp edge of the amorphous layer possibly because of less entanglement of the PEO chains with a relatively low molecular weight.

3.3. Gap distances

From the surface profile II shown in Fig. 3, the region marked by an arrow clearly shows that there is a narrow gap rather than continuum between the amorphous layer and the outermost tip of the crystal pattern, indicating that macromolecules in the amorphous layer must migrate through the depletion zone before they join the crystals. The gap distances between the outermost growing tips of the crystal pattern and the nearest edge of the amorphous layer were determined from all the images, and the results are shown in Fig. 4. Gaussian function was used to fit the results. The average distance is about 253 nm.

3.4. Radius of gyration of PEO in amorphous layer and gap distance

The gyration radius, $\overline{R}_g^s$, of this PEO in water was measured using laser light scattering. Since water is a relatively good solvent for PEO, the interactions among PEO segments could be similar to those between water and PEO repeating units, so it is reasonable to make a hypothesis that the chain

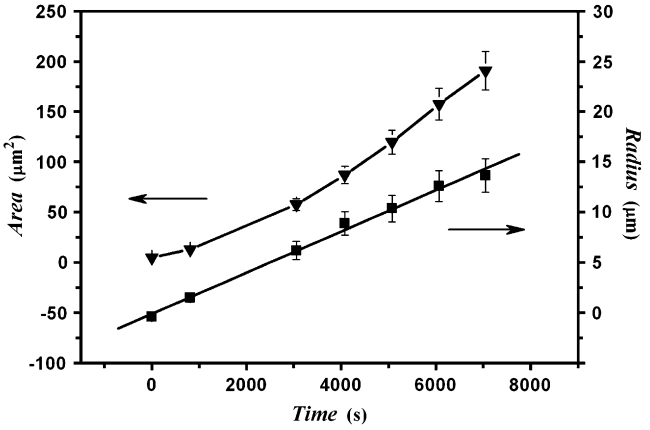

Fig. 2. Plots of area and radius versus time: ■ represents radius on the right scale; ▼ represents area (not containing the depletion zone) on the left scale.

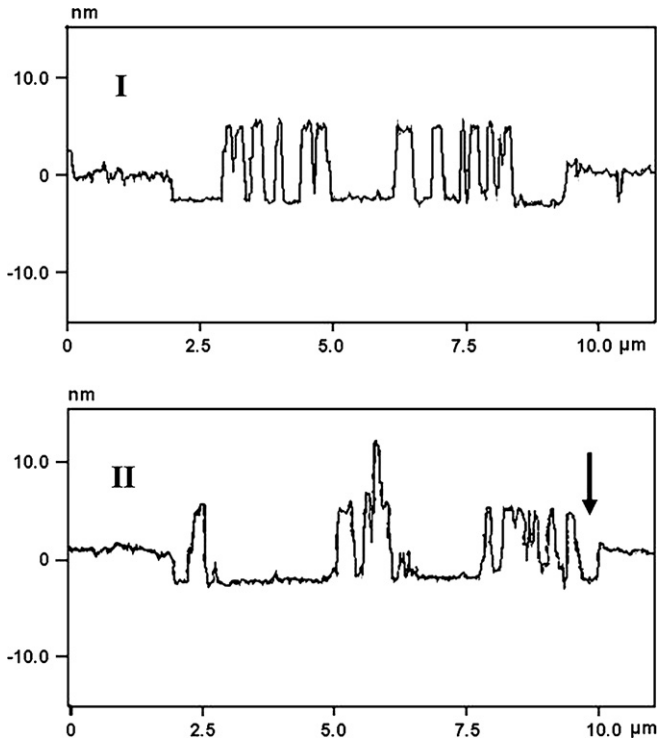

Fig. 3. Two typical surface profiles of the growth patterns shown in Fig. 1(b). They show the thicknesses of the crystal and the amorphous layer, and the gap distances between the crystal and the amorphous layer.

conformation in amorphous state is similar to that in water solution, that is, $\overline{R}_g^m \approx \overline{R}_g^s$. Further assuming that the volume change caused by the strong attraction of substrate is negligible, the relationship of $4/3\overline{R}_g^{w^3}\pi \approx \overline{R}_g^{l2}H\pi$ can be obtained. The formula on the left side is the average spherical volume of PEO macromolecules in water with $\overline{R}_g^s = 50.2$ nm, while the one on the right side is the volume of a round "disk" on the substrate with the thickness $H = 3$ nm and a gyration radius, $\overline{R}_g^l$. Then, the radius of the "disk" on the substrate is calculated to be $\overline{R}_g^l = 237$ nm. Interestingly, this value is quite close to the average shortest gap distance of 253 nm [35]. This further implies that the diffusion distances for the molten molecules are not too long, only the gyration radius, $\overline{R}_g^l$, in PEO thin layer with a 3 nm thickness.

3.5. Fractal crystal formation process

It is well known that the formation of these highly ramified patterns is generally due to the instability of crystal growth in the nonequilibrium condition [4,5]. The seaweed patterns, which we obtained, have a fractal dimension of $D_f \approx 1.63$ and are quite similar to the simulation results using the classical DLA model without considering any boundary condition [6]. This further means that these seaweed patterns were formed in a diffusion-controlled condition.

In Fig. 5(a) the crystallization process is schematically described, which is as follows: disentanglement from the deformed PEO layer, migration process via the depletion zone, and finally joining the growing crystal in the areas near tips. According to our statistical result shown in Fig. 4, the shortest gap distance between the growing tips and the amorphous layer edge is 253 nm on average. This is the distance that the molten molecules have to cross to join crystals. It is possible that the process of the PEO chains diffusing through the depletion zone is the key step, so results in instability of the crystal growth. Finally, the resultant patterns have the fractal feature.

Fig. 5(b) schematically shows a top view of the growing tips and the distribution of molten PEO molecules in the amorphous layer. Obviously, the gap distance increases away from the growing tips. This increase means that crossing the gap becomes more difficult. Assuming that the diffusion in the depletion zone is the key step, a flow of molecules in the amorphous layer may occur to get the shortest diffusion distance over the gaps. This will result in a fast growth of the patterns mainly in the areas around active tips. So, the width of the branches is narrower than the distance between two adjacent branches. As a result, the pattern has a relatively non-dense morphology.

The growth described in Fig. 5(b) cannot be straightforward. In the case that the growing tip absorbs a large number of the molten molecules in opposite amorphous layer, the distance between the tip and the amorphous layer may be no longer shortest, the tip growth can slow down gradually and finally ceases. The shortest gap distances can appear at an area away from the growth-stopping tip's top, so new tips will emerge at the area and then grow at a direction different from the previous tip. This causes the formation of ramified pattern.

3.6. Time-dependent radius of the crystal pattern

Pattern growth kinetics at the supercooling condition has been studied in both experiment [17,19,36] and simulation [24]. The experimental investigations show the linear, $R(t) \propto t^1$ [17], and non-linear, $R(t) \propto t^{0.5}$ [19,36], relations between pattern radius and time found from different polymers at the different supercooling conditions. The theoretical simulation confirms that the growth of crystal patterns is a surface kinetic process, that is, a linear growth [24]. In our study, we have obtained a linear radius growth, $R(t) \propto t^1$, in the

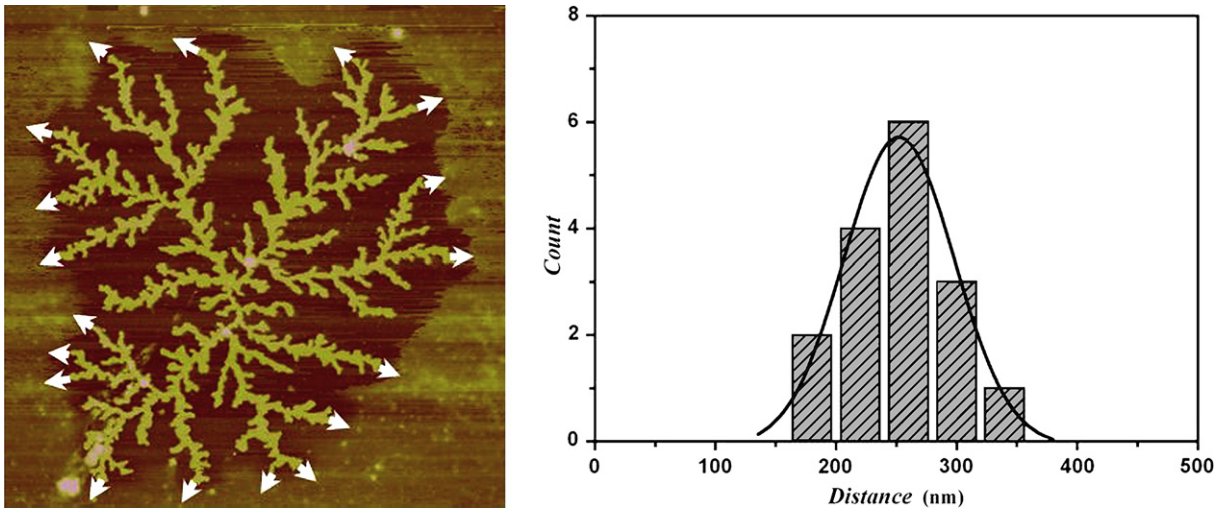

Fig. 4. Gap distances between the amorphous layer and the outermost growing tips.

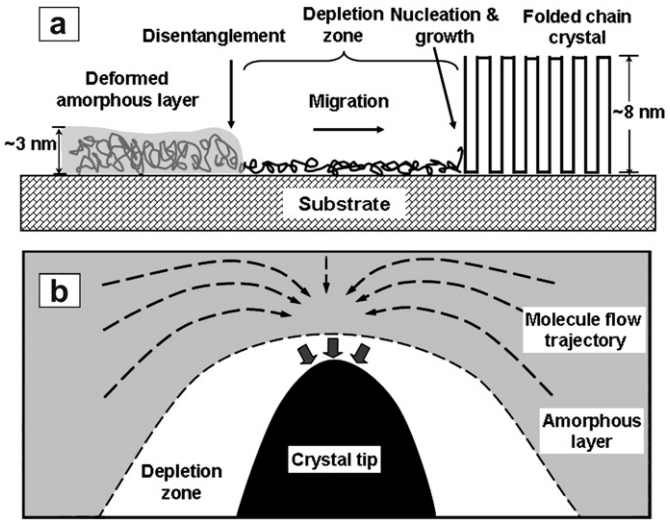

Fig. 5. Side (a) and top (b) views of the crystal growth process.

time regime used. This experimental result is consistent with those found in the thin film samples of an isotactic polystyrene [17] and predicted by simulation [24]. So, we believe that the surface kinetic process controls the growth rate of crystals in our system. Seemingly, this conclusion is contrary to the fractal feature of these crystal patterns created via diffusion-controlled process. Actually, the determined radius of the ramified crystals is similar to that of spherulites which also show a $R(t) \propto t^1$ relation. It is well known that the spherulite growth is controlled by a diffusion process. In other words, the $R(t) \propto t^1$ relation is not associated with the fractal feature of growing crystal patterns. In fact, the fractal feature is reflected by creating an edge which is much longer than that being able to be described by *Euclidean* geometry.

4. Conclusion

In summary, we have carried out an in situ observation of the fractal crystal pattern growth process from a thin amorphous layer of a high molecular weight PEO at 25 °C using atomic force microscopy with a hot stage. The significant achievement is to experimentally find a depletion zone between the ramified crystal pattern and the highly viscous amorphous layer. Meanwhile, we found that the gap distance between the growing tips and the edge of the amorphous layer is about 253 nm, which is close to the gyration radius of the PEO chains in the thin layer. The existence of the depletion zone means that the PEO chains have to diffuse through the zone to join crystals. This diffusion-controlled process explains the mechanism of the fractal pattern formation. The linear relation between the pattern radius and time illustrates the surface kinetic process controlling the crystal growth.

Acknowledgement

Financial supports given by Nankai University for start-up funding and the National Science Foundation of China for a grant (NSFC20474033) are gratefully acknowledged.

References

[1] Bassett BC. Principles of polymer morphology. Cambridge: Cambridge University Press; 1981.
[2] Wunderlich B. Macromolecular physics, vols. 1 and 2. New York: Academic; 1976.
[3] Schultz JM. Polymer crystallization. New York: Oxford University Press; 2001.
[4] Langer JS. Rev Mod Phys 1984;52:1–28.
[5] Meakin P. Fractals, scaling and growth far from equilibrium. Cambridge: Cambridge University Press; 1997.
[6] Witten Jr TA, Sander LM. Phys Rev Lett 1981;47:1400–3; Witten Jr TA, Sander LM. Phys Rev B 1983;27:5686–97.
[7] Deutscher G, Lereah Y. Phys Rev Lett 1988;60:1510–3.
[8] Couder Y, Argoul F, Arnéodo A, Maurer J, Rabaud M. Phys Rev A 1990;42:3499–503.
[9] Hwang RQ, Schröder J, Günther C, Behm R. Phys Rev Lett 1991; 67:3279–82.
[10] Lereah Y, Deutscher G, Grünbaum E. Phys Rev A 1991;44: 8316–22.

[11] Lereah Y, Zarudi I, Grünbaum E, Deutscher G, Buldyrev SV, Standely HE. Phys Rev E 1994;49:649–56.
[12] Utter B, Ragnarsson R, Bodenschatz E. Phys Rev Lett 2001;86:4604–7.
[13] Keith HD, Padden FJ. J Appl Phys 1964;35:1270–85.
[14] Lovinger AJ, Cais RE. Macromolecules 1984;17:1939–45.
[15] Reiter G, Sommer J-U. Phys Rev Lett 1998;80:3771–4.
[16] Reiter G, Sommer J-U. J Chem Phys 2000;112:4376–83.
[17] Taguchi K, Miyaji H, Izumi K, Hoshino A, Miyamoto Y, Kokawa R. Polymer 2001;42:7443–7.
[18] Wang M, Braun HG, Meyer E. Macromolecules 2004;37:437–45.
[19] Mareau VH, Prud'homme RE. Macromolecules 2005;38:398–408.
[20] Zhai X-M, Wang W, Zhang G-L, He B-L. Macromolecules 2006; 39:324–9.
[21] Vicsek T. Phys Rev Lett 1984;53:2281–4;
Vicsek T. Phys Rev A 1985;32:3084–9.
[22] Banavar JR, Kohmoto M, Roberts J. Phys Rev A 1986;33:2065–7.
[23] Aukrust T, Novotny MA, Browne DA, Kaski K. Phys Rev A 1989; 39:2587–92.
[24] Saito Y, Ueta T. Phys Rev A 1989;40:3408–19.
[25] Eckmann J-P, Meakin P, Procaccia I, Zeitak R. Phys Rev Lett 1990; 65:52–5.
[26] Yokoyama E, Kuroda T. Phys Rev A 1990;41:2038–49.
[27] Ohta S, Honjo H. Phys Rev A 1991;44:8425–8.
[28] Ihle T, Müller-Krumbhaar H. Phys Rev Lett 1993;70:3083–6.
[29] Brener E, Müller-Krumbhaar H, Temkin D. Phys Rev E 1996; 54:2714–22.
[30] Bogoyavlenskiy VA, Chernova NA. Phys Rev E 2000;61:1629–33.
[31] Sommer J-U, Reiter G. J Chem Phys 2000;112:4384–93.
[32] Cheng SZD, Chen J, Janimak JJ. Polymer 1990;31:1018–24.
[33] Sukhishvili SA, Chen Y, Müller JD, Gratton E, Schweizer KS, Granick S. Nature 2000;406:146.
[34] Hobbs J. In: Reiter G, Strobl G, editors. Progress in understanding of polymer crystallization. Berlin, Heidelberg: Springer; 2007.
[35] It is worth to mention that the closeness was obtained on the base of the two hypotheses. To confirm that it is not a coincidence it needs to perform further theoretical and experimental studies.
[36] Zhu DS, Liu YX, Chen EQ, Li M, Chen C, Sun YH, et al. Macromolecules 2007;40:1570–8.